SPEKTRA: Jurnal Fisika dan Aplikasinya
Volume 10, Issue 2, August 2025
Homepage: doi.org/10.21009/SPEKTRA

DOI: doi.org/10.21009/SPEKTRA.102.06

Analysis of the Effect of ZnO, FeO, MnO, and MgO Dopants on the Optical Properties of P_2O5-CaO Glass System and Comparison With P_2O_5-Eggshell Glass System

Haifany[1,*], Eka Laela Nun Karina[1], Selsa Sururiyah Sya'baniah[1], Zahra Sajidah Hariyawan[1], Haryanto[1], Agus Setyo Budi[1], Anggara Budi Susila[1], Hadi Nasbey[1]

[1]*Department of Physics, FMIPA, Universitas Negeri Jakarta, DKI Jakarta, Indonesia*

*Corresponding Author Email: haifany_1306621076@mhs.unj.ac.id

Received: 20 May 2025
Revised: 31 July 2025
Accepted: 16 August 2025
Online: 30 August 2025
Published: 31 August 2025

SPEKTRA: Jurnal Fisika dan Aplikasinya
p-ISSN: 2541-3384
e-ISSN: 2541-3392

ABSTRACT

This study investigates the effect of ZnO, FeO, MnO, and MgO dopants on the optical properties of phosphate-based glass within the P_2O_5–CaO system and compares the results with glasses using eggshell-derived CaO as an alternative calcium source. The glass samples were synthesized using the melt quenching method, followed by characterization using Energy Dispersive X-ray (EDX) and UV-Visible spectroscopy. EDX analysis confirmed that phosphorus and oxygen were the dominant elements in all samples, with successful incorporation of each dopant as a network modifier. UV-Vis analysis revealed that the optical properties of the glass were significantly affected by both dopant type and concentration. The addition of ZnO decreases absorbance and widens the band gap up to 10 mol%, indicating improved structural regularity of the glass network. MnO exhibits a non-linear trend, with the highest absorbance observed at 5 mol% and decreasing at higher concentrations. The band gap varies from 3.37 eV to 3.59 eV, suggesting a transition from a disordered to a more stable and compact glass structure. In contrast, FeO and MgO doping reduced the band gap energy due to increased formation of non-bridging oxygen and network disruption. Additionally, comparison with eggshell-derived CaO showed higher UV absorbance compared to glass made with pure CaO, especially in the wavelength range below 400 nm, indicating that the raw material source influences the optical performance of the glass. Overall, this research highlights the potential of tuning dopant concentration and

utilizing sustainable raw materials to enhance the optical characteristics of phosphate glass for use in UV-blocking, optoelectronic, and sensor applications.

Keywords: phosphate glass, metal oxide, ZnO, MgO, MnO, FeO, calcium oxide, eggshell, optical properties

INTRODUCTION

Phosphate-based glass (P_2O_5) is a type of inorganic material that has attractive characteristics such as high optical transparency, low coefficient of thermal expansion, and the ability to form stable glass networks [1]. Phosphate glass also has the ability to be structurally modified through the addition of various metal oxide compounds, which makes it a potential candidate in optoelectronic applications, anti-UV coatings and optical sensors [2]. One important modification that is often done is to add calcium oxide (CaO) compounds as a network modifier to lower the melting point of the glass [3]. Metal oxide doping such as ZnO, FeO, MnO, and MgO is also widely used to improve the optical and electrical properties of glass. Each type of dopant has unique characteristics that can affect the formation of bridging oxygen (BO) and non-bridging oxygen (NBO) in the glass network, thus having a direct impact on changes in bandgap energy values and light absorption capabilities[4].

In addition to using pure chemicals, a more environmentally friendly approach has also begun to be developed through the utilization of organic waste as a source of raw materials [5]. One example is eggshells, which contain large amounts of calcium carbonate ($CaCO_3$) and can be calcined into CaO [6]. The use of eggshells as an alternative raw material for glass not only supports the concept of green materials, but also has the potential to reduce production costs [7]. Therefore, a cdinignomparative study between P_2O_5-CaO-based glass systems and P_2O_5-eggshell-based glass systems is relevant to assess the feasibility and effectiveness of such substitution.

This study aims to analyze the effect of variations in the concentration of ZnO, FeO, MnO, and MgO dopants on the optical properties of P_2O_5-CaO glass systems and compare them with glass systems that use eggshells as a source of calcium. The results of this study are expected to contribute to the development of phosphate-based functional glass materials with improved optical properties while supporting the utilization of organic waste as a sustainable alternative material. However, limited studies have compared the optical behavior of phosphate glasses synthesized using eggshell-derived CaO as a sustainable calcium source, particularly when combined with different transition metal oxide dopants. The present work aims to fill this gap by demonstrating how eggshell-based CaO influences the structural and optical response of doped phosphate glass, providing both scientific insight and an environmentally friendly alternative to conventional chemical precursors.

METHODS

This study uses the melt quenching method to synthesize glass with P_2O_5-CaO composition and variations of ZnO, FeO, MnO, and MgO dopants. The raw materials were weighed according to the mole composition, mixed evenly, and then melted in a furnace at 900-1100°C for about 1 hour. The glass melt is then poured onto a metal plate for rapid cooling (quenching). After cooling, the samples were crushed and ground to a fine glass powder for characterization purposes. Optical tests were performed using a UV-Vis spectrophotometer in the wavelength range of 200-800 nm, and absorbance data were analyzed using the Tauc plot method to determine the optical gap energy (bandgap) value. The value of material composition in mass units can be calculated using the formula [8]:

$$MW = (mol\% \times Mr) + (mol\% \times Mr) + (mol\% \times Mr), \quad (1)$$

$$WP_{material} = Material(mol\%) \times \frac{Mr}{MW} \times 100\%, \quad (2)$$

$$m_{material} = WP_{material} \times 15\ gram, \quad (3)$$

where m is the mass of the composition of each material, WP is the weight percent of the composition used, while m_{total} is the total mass of all compositions used. The equation for calculating the energy gap is as follows [9]:

$$(\alpha hv)n = B(hv - Eg). \quad (4)$$

Photon energy (eV) is obtained by the formula:

$$hv = E = \frac{hc}{\lambda} \quad (5)$$

where h is Planck's constant, c is the speed of light, and λ is the wavelength. By plotting $(\alpha hv)^2$ versus hv, the band gap energy was determined from the intercept of the linear portion of the graph with the energy axis. Error margins in band gap values were calculated within ±0.02 eV, based on repeated measurements from three replicate spectra [10].

RESULTS AND DISCUSSIONS

EDX characterization results

1. (65-x)P2O5-xZnO-35CaO glass system with 10% mol ZnO dopping concentration

TABLE 1 shows that the main elements in the glass samples are oxygen (43.48%) and phosphorus (34.61%), which confirms the dominance of P_2O_5 as the forming glass network [11]. The Zn content of 9.81% proves the success of ZnO doping as a modifier that simplifies the polyphosphate structure [12], while Ca (9.69%) plays a role in lowering the melting point [13]. Al and Si signals were detected in small amounts (<2%) which are thought to come from contamination of the synthesis process, so they have no significant effect on the glass structure.

TABLE 1. The EDS results on (65-x)P_2O_5-xZnO-35CaO glass samples with 10 mol% ZnO doping show the mass composition (Wt%) and atomic composition (At%) of each element.

Element	Elemental Mass Composition (Wt%)	Elemental Atomic Composition (At%)
O	43.48	63.01
P	34.61	25.90
Zn	09.81	03.48
Ca	09.69	05.61
Si	01.79	01.48
Al	00.61	00.53

2. (70-X)P_2O_5-xMgO-30CaO glass system with 10% mol MgO dopping concentration

TABLE 2 show that the main constituents of the glass are O (40.81%), P (36.25%), Ca (10.37%), and Mg (4.02%), in accordance with the composition of the 30CaO-xMgO-(70-x)P_2O_5 system. The presence of minor elements such as Co, Si, In, and Al in concentrations below 5% is thought to come from contamination of the preparation process, do not significantly affect the optical or structural properties of the glass. The presence of Mg^{2+} confirms the success of the doping process, as this ion acts as a network modifier that regulates the ratio of bridging and non-bridging oxygen, thus affecting the optical characteristics of the material [14].

TABLE 2. The EDS results on (70-X)P_2O_5-xMgO-30CaO glass samples with 10 mol% MgO doping show the mass composition (Wt%) and atomic composition (At%) of each element.

Element	Elemental Mass Composition (Wt%)	Elemental Atomic Composition (At%)
O	40.81	58.96
P	36.25	27.05
Ca	10.37	5.98
Mg	4.02	3.82
Co	2.02	0.79
Si	2.06	1.70
In	3.25	0.65
Al	1.21	1.04

3. (70-x)P_2O_5-xFeO-30CaO glass system with 5% mol FeO dopping concentration

TABLE 3 shows that the main elements in the glass sample are oxygen (40.34%) and phosphorus (37.22%), confirming the dominance of P_2O_5 as the primary glass former in the phosphate-based network [15]. The presence of Fe at 5.19% indicates successful doping of FeO as a network modifier, which is expected to influence the optical properties by introducing localized states in the band structure. Calcium (10.59%) also acts as a modifier that contributes to structural stability and reduces the melting point of the glass. Minor elements such as Na (0.48%), Mg (0.52%), Al (1.40%), and Si (4.26%) were detected in low concentrations (<5%), likely originating from impurities or contamination during the synthesis process, and are not expected to significantly affect the overall glass network.

TABLE 3. The EDS results on (70-x)P_2O_5-xFeO-30CaO glass samples with 5 mol% FeO doping show the mass composition (Wt%) and atomic composition (At%) of each element.

Element	Elemental Mass Composition (Wt%)	Elemental Atomic Composition (At%)
O	40.34	58.29
Fe	05.19	02.15
Na	00.48	00.48
Mg	00.52	00.49
Al	01.40	01.20
Si	04.26	03.51
P	37.22	27.78
Ca	10.59	06.11

4. (70-x)P2O5-xMnO-30CaO glass system with 10% mol MnO dopping concentration

TABLE 4 presents the EDX analysis of the MnO glass system, which shows oxygen (35.06 wt%) and phosphorus (28.92 wt%) as the dominant elements, confirming the formation of a phosphate glass matrix. Mn (9.62 wt%) is successfully incorporated as a dopant, while Ca (9.14 wt%) acts as a stabilizer [16]. Minor elements like C, Si, Al, and Mg may originate from raw materials or equipment. The composition supports the intended MnO doping in the glass network.

TABLE 4. The EDS results on (70-x)P_2O_5-xMnO-30CaO glass samples with 10 mol% MnO doping show the mass composition (Wt%) and atomic composition (At%) of each element.

Element	Elemental Mass Composition (Wt%)	Elemental Atomic Composition (At%)
C	14.27	24.62
O	35.06	45.42
Mg	00.23	00.19
Al	00.70	00.53
Si	02.08	01.53
P	28.92	19.35
Ca	09.14	04.72
Mn	09.62	03.63

5. 60P2O5-40CaO glass system

TABLE 5 presents the EDX analysis of the CaO glass system, showing that the main elements are phosphorus (29.39 wt%), carbon (22.15 wt%), oxygen (18.66 wt%), and calcium (17.91 wt%), which confirms the presence of phosphate and CaO as the key components. Minor elements like cerium (7.21 wt%), silicon, zinc, and aluminum are also detected, possibly from dopants or raw material impurities. The overall composition indicates a stable glass structure with potential optical activity [17].

TABLE 5. The EDS results on $60P_2O_5$-40CaO show the mass composition (Wt%) and atomic composition (At%) of each element.

Element	Elemental Mass Composition (Wt%)	Elemental Atomic Composition (At%)
C	22.15	40.19
O	18.66	25.43
Zn	01.80	00.60
Al	00.37	00.30
Si	02.51	01.94
P	29.39	20.68
Ca	17.91	09.74
Ce	07.21	01.12

Absorbance and Band Gap Result

1. (65-x)P2O5-xZnO-35CaO glass system with 0-15% mol ZnO dopping concentration

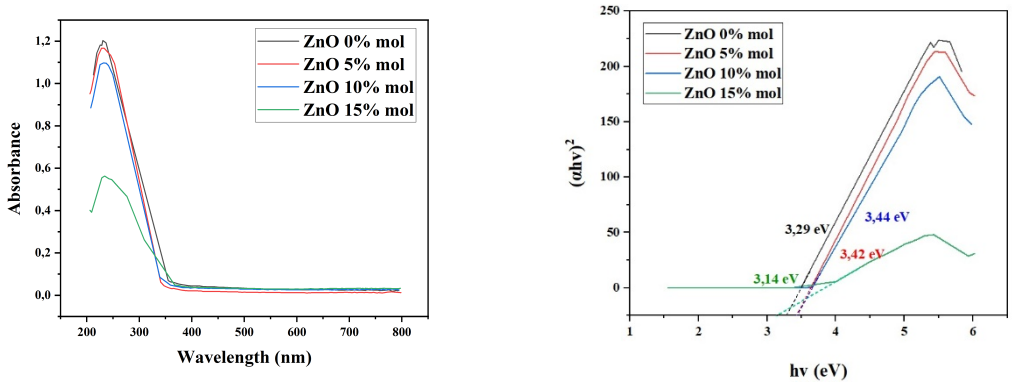

(a) (b)

FIGURE 1. (a) Absorbance spectra of (65-x)P_2O_5-xZnO-35CaO glass system with varying ZnO concentrations (0–15 mol%) in the wavelength range of 200–800 nm. (b) Tauc plot used to estimate the optical band gap energy of each sample.

Based on the FIGURE 1, show that all glass samples have high absorbance in the ultraviolet region (200-350 nm) with a maximum peak in the samples without ZnO, while an increase in ZnO concentration leads to a decrease in absorbance and a shift in the absorption peak to larger wavelengths. This trend indicates that ZnO dopants affect the regularity of the glass network structure, reduce optical defects that become light absorption centers, and improve matrix homogeneity [17]. The addition of ZnO up to 10% mole increases the energy bandgap due to the strengthening of network bonds and the reduction of defect states, while the concentration of 15% mole decreases the bandgap to 3.14 eV due to the formation of local energy levels that facilitate electronic transitions [18] and the effect of BO-NBO ratio on absorption characteristics [19], so the control of ZnO doping is key to the stability of the optical properties of the glass.

2. (70-X)P2O5-xMgO-30CaO glass system with 0-15% mol MgO dopping concentration

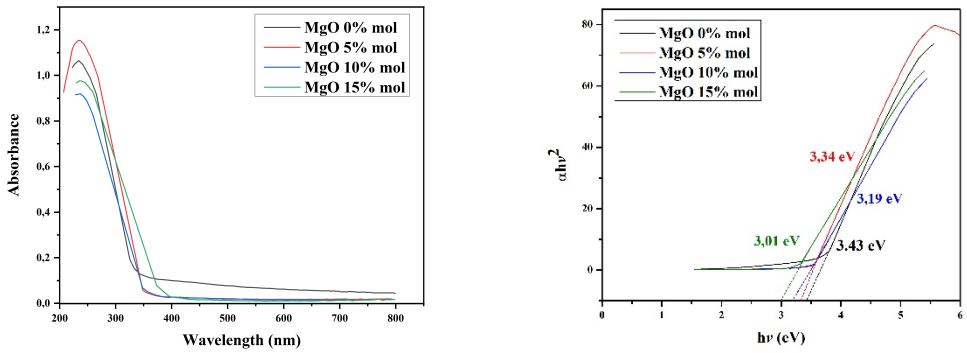

(a) (b)

FIGURE 2. (a) Absorbance spectra of (70-X)P_2O_5-xMgO-30CaO glass system with varying MgO concentrations (0–15 mol%) in the wavelength range of 200–800 nm. (b) Tauc plot used to estimate the optical band gap energy of each sample.

Based on the FIGURE 2, analysis of the absorbance graph of phosphate glass with varying MgO concentrations shows that the absorbance characteristics change with increasing concentration. Samples without MgO have an absorbance peak at a wavelength of 230–270 nm with a maximum value of approximately 1.05. The addition of 5% MgO increases the absorbance to approximately 1.13. However, at a concentration of 10%, the absorbance value decreases to approximately 0.90 [20]. Meanwhile, at 15%, the absorbance slightly increases to 0.96, but adjustments to temperature and heating time are required due to increased viscosity that hinders the melting process. After adjustments are made, the graph shows stable results with good transparency above a wavelength of 350 nm. The graph shows that the optical band gap value decreases as the MgO concentration increases. Glass without MgO has the highest band gap of 3.43 eV, while doping with 5%, 10%, and 15% respectively reduces the band gap value to 3.34 eV, 3.19 eV, and 3.01 eV [21].

3. (70-x)P2O5-xFeO-30CaO glass system with 0-15% mol FeO dopping concentration

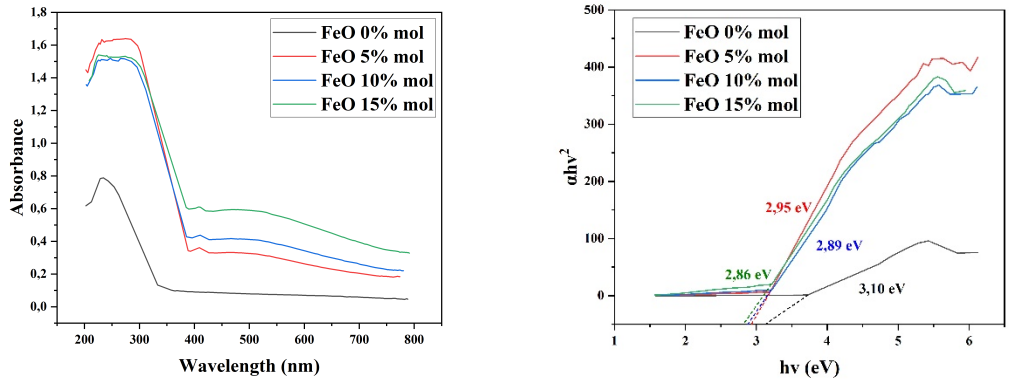

(a) (b)

FIGURE 3. (a) Absorbance spectra of (70-x)P_2O_5-xFeO-30CaO glass system with varying FeO concentrations (0–15 mol%) in the wavelength range of 200–800 nm. (b) Tauc plot used to estimate the optical band gap energy of each sample.

Based on the FIGURE 3, The absorbance and optical band gap graphs of phosphate glass with varying FeO concentrations demonstrate that FeO addition significantly influences the material's optical properties. Absorbance increases sharply from approximately 0.8 (FeO 0% mol) to around 1.6 at 5% mol concentration, then slightly decreases at 10% and 15% mol, yet remains higher than the undoped sample. This indicates that Fe^{2+} ions act as absorption centers that enhance electronic transitions. Meanwhile, the Tauc plot shows a decrease in the band gap energy from 3.10 eV (FeO 0%) to 2.95 eV (5%), 2.89 eV (10%), and 2.86 eV (15%), suggesting that increasing FeO content leads to the formation of non-bridging oxygen (NBO) and network disruption, which lowers the minimum energy required for electronic excitation, in accordance with the glass network depolymerization [22].

4. (70-x)P2O5-xMnO-30CaO glass system with 0-15% mol MnO dopping concentration

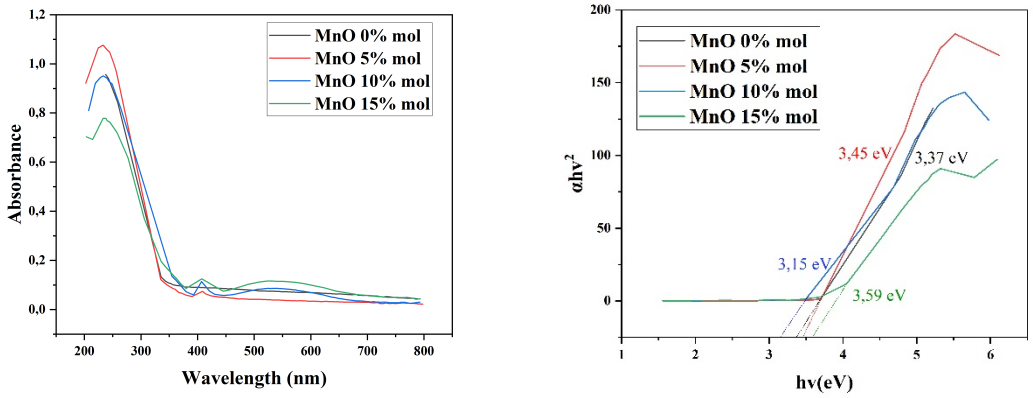

(a) (b)

FIGURE 4. (a) Absorbance spectra of (70-x)P_2O_5-xMnO-30CaO glass system with varying MnO concentrations (0–15 mol%) in the wavelength range of 200–800 nm. (b) Tauc plot used to estimate the optical band gap energy of each sample.

Based on the FIGURE 4, the glass sample with 5% MnO exhibits the highest absorbance, peaking at around 270 nm, indicating enhanced UV absorption. As the MnO concentration increases beyond 5%, the absorbance gradually decreases, with the 15% MnO sample showing the lowest intensity. This trend suggests that low concentrations of MnO effectively disrupt the glass network, increasing light absorption, while higher concentrations may lead to structural stabilization or ion clustering that reduces absorbance. All samples show significant absorption in the UV region (200–300 nm), confirming their potential for UV-blocking applications [23]. Overall, MnO concentration plays a crucial role in tuning the optical response of phosphate glass. Based on the Tauc plot shown, the optical band gap values of phosphate glass samples vary with MnO concentration. The undoped sample (0% MnO) has a band gap of 3.37 eV, which slightly decreases to 3.45 eV at 5% MnO and further drops to 3.15 eV at 10% MnO, indicating the formation of non-bridging oxygen and structural disorder that narrows the energy gap. Interestingly, at 15% MnO, the band gap increases to 3.59 eV, suggesting a restructuring of the glass network into a more compact and ordered form. This

non-linear trend confirms that MnO acts not only as an optical dopant but also influences the structural stability of the glass matrix, allowing band gap tuning for specific UV-optical applications [11].

5. P2O5-CaO glass system with a comparison of pure CaO and eggshell-derived CaO in the range of 25–40% mol

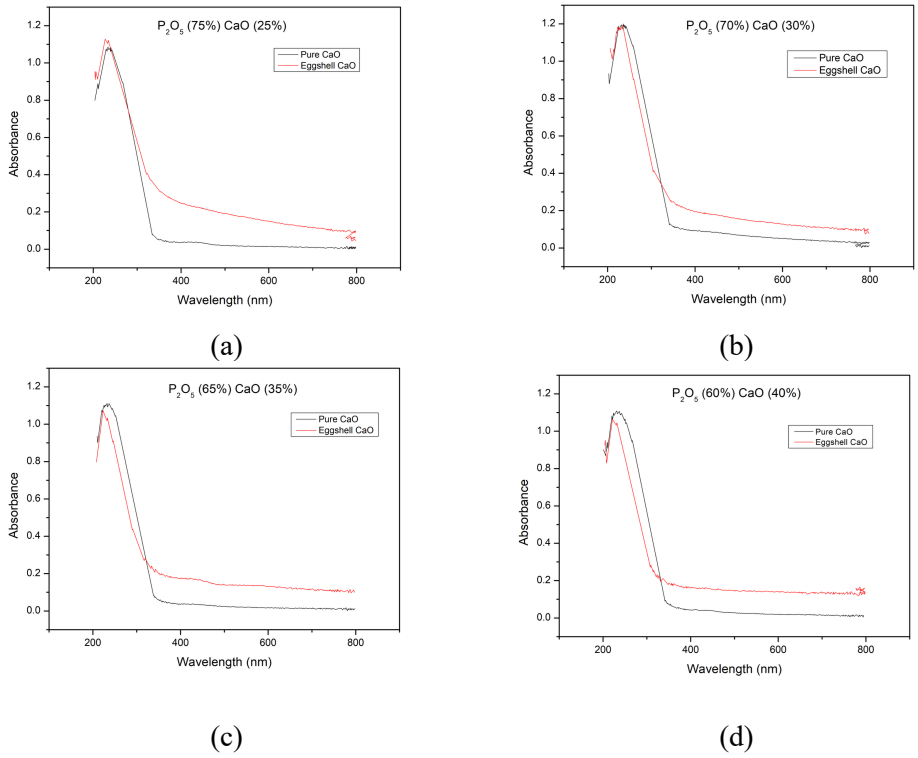

FIGURE 5. Absorbance spectra of P_2O_5–CaO glass with a comparison between pure CaO and eggshell-derived CaO at various compositions: (a) P_2O_5 (75%)–CaO (25%), (b) P_2O_5 (70%)–CaO (30%), (c) P_2O_5 (65%)–CaO (35%), and (d) P_2O_5 (60%)–CaO (40%).

Based on the UV-Vis spectra (FIGURE 5), samples with eggshell-derived CaO (red line) generally show higher absorbance than those with pure CaO (black line), especially below 400 nm. The absorbance difference is notable at 25% CaO, decreases at 30% and 35%, then increases again at 40%. This indicates that the source of CaO affects the optical absorption of the glass. Overall, increasing CaO content tends to reduce absorbance, but the influence of the CaO source remains consistent [24].

FIGURE 6 shows a comparison of the band gap values, revealing that samples containing eggshell-derived CaO consistently exhibit higher band gap energies than those with pure CaO across all compositions (25–40%). The band gap of eggshell CaO increases with CaO content, reaching a peak at 35%, before slightly decreasing at 40%. In contrast, pure CaO samples show a relatively lower and less variable band gap trend. These findings suggest that the origin of CaO significantly influences the electronic structure of the glass, likely due to differences in impurities or structural modifiers present in the raw materials [25].

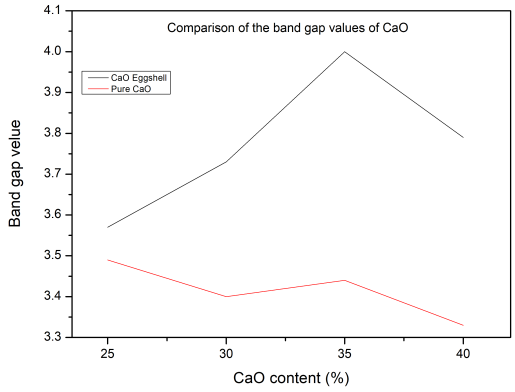

FIGURE 6. Band gap comparison of pure CaO and eggshell-derived CaO at different CaO contents.

CONCLUSION

This study examined the effects of ZnO, FeO, MnO, and MgO dopants on the optical properties of P_2O_5–CaO glass and compared them with glass made using eggshell-derived CaO. EDX results confirmed the dominance of P_2O_5 and the successful incorporation of dopants as network modifiers. UV-Vis analysis showed that ZnO and MnO improve absorbance and band gap up to optimal concentrations, while higher levels lead to structural stabilization or defect formation. FeO and MgO doping reduced the band gap due to increased non-bridging oxygen and network disruption. Glasses using eggshell-based CaO showed higher UV absorbance than those using pure CaO, confirming the influence of raw material sources on optical behavior. Dopant concentration and CaO source significantly affect the optical properties of phosphate glass, offering potential for tailored applications and sustainable material development.

ACKNOWLEDGMENTS

The authors would like to express their sincere gratitude to the Laboratory of Inorganic Materials, Department of Physics, for providing the necessary facilities and technical support during the research process. We also thank the research team members and academic supervisors for their valuable guidance and constructive feedback. Special appreciation is extended to those who contributed to the synthesis, characterization, and analysis of the glass samples. This research would not have been possible without your support.

REFERENCES

[1] A. M. Aliyu and N. E. Ahmed, “Structure and physical properties of $30MgSO_4$-$(70–x)$ P_2O_5-xSm_2O_3 glasses,” *Educatum J. Sci. Math. Technol.*, vol. 6, no. 2, pp. 22–34, Dec. 2019, doi: 10.37134/ejsmt.vol6.2.3.2019.

[2] Y. Lai et al., "Recent Advances in TiO_2-Based Nanostructured Surfaces with Controllable Wettability and Adhesion," *Small*, vol. 12, no. 16, pp. 2203–2224, 2016, doi: 10.1002/smll.201501837.

[3] J. Jiusti et al., "Effect of network formers and modifiers on the crystallization resistance of oxide glasses," *J. Non Cryst. Solids*, vol. 550, no. August, p. 120359, 2020, doi: 10.1016/j.jnoncrysol.2020.120359.

[4] A. M. Fayad, M. A. Ouis, R. M. M. Morsi, and R. L. Elwan, "Enhancement of electrical conductivity associated with non-bridged oxygen defects in molybdenum phosphate oxide glass via doping of SrO," *Sci. Rep.*, no. 0123456789, pp. 1–14, 2023, doi: 10.1038/s41598-023-45333-7.

[5] B. Sharma, B. Vaish, M. Umesh, K. Singh, P. Singh, and R. Pratap, "Recycling of Organic Wastes in Agriculture: An Environmental Perspective," *Int. J. Environ. Res.*, no. 0123456789, 2019, doi: 10.1007/s41742-019-00175-y.

[6] L. Izzati, S. Rahayu, and D. W. Kurniawii, "Identifikasi karakteristik serbuk kalsium karbonat ($CaCO_3$) dari cangkang kerang mutiara (*Pinctada maxima*)," *Indonesian Phys. Rev.*, vol. 5, no. 2, pp. 130–136, 2022.

[7] B. Ngayakamo and A. P. Onwualu, "Recent advances in green processing technologies for valorisation of eggshell waste for sustainable construction materials," *Heliyon*, vol. 8, no. 6, p. e09649, 2022, doi: 10.1016/j.heliyon.2022.e09649.

[8] A. Shivapuji, *Estimation of Molecular Weight Knowing the Mixture Composition and Conversion of Mole Fraction to Mass Fraction and Vice Versa*. Self-published, Aug. 2019, doi: 10.13140/RG.2.2.31457.45926.

[9] N. Y. Aldaleeli, M. Madani, S. A. Al-Gahtany, H. Elhaes, R. Badry, and M. A. Ibrahim, "Evaluation of Different Concentrations of Graphene on the Structural and Optical Properties of Carboxymethyl Cellulose Sodium," *Polymers (Basel)*, vol. 17, no. 3, pp. 1–19, 2025, doi: 10.3390/polym17030391.

[10] D. Yuan and Q. Liu, "Photon energy and photon behavior discussions," *Energy Reports*, vol. 8, no. November, pp. 22–42, 2022, doi: 10.1016/j.egyr.2021.11.034.

[11] Y. Alaoui, M. El Moudane, A. Er-rafai, M. Khachani, A. Ghanimi, A. Sabbar, M. Tabyaoui, A. Guenbour, and A. Bellaouchou, "Structural study, thermal and physical properties of K_2O-CaO-P_2O_5 phosphate glasses," *Moroccan Journal of Chemistry*, vol. 9, no. 3, Aug. 2021, doi: 10.48317/IMIST.PRSM/morjchem-v9i2.22505.

[12] J. Schwarz, H. Tichá, L. Tichý, and R. Mertens, "Physical properties of PbO–ZnO–P_2O_5 glasses: I. Infrared and Raman spectra," *Journal of Optoelectronics and Advanced Materials*, vol. 6, no. 3, pp. 737–746, Sep. 2004.

[13] M. Tarrago, I. Royo, S. Martínez, M. Garcia-Valles, and D. R. Neuville, "Incorporation of calcium in glasses: A key to understand the vitrification of sewage sludge," *Int. J. Appl. Glass Sci.*, vol. 12, no. 3, pp. 367–380, Jul. 2021, doi: 10.1111/ijag.15920.

[14] M. P. Amanda, Budhijanto, and G. A. S. Ramadhani, "Analisis Pengaruh Penambahan Magnesium Oksida terhadap Sifat Mekanis Bioadhesif Berbasis Kitosan-Karagenan," *Jurnal Teknik Kimia USU*, vol. 13, no. 1, pp. 54–62, Mar. 2024, doi: 10.32734/jtk.v13i1.14656.

[15] G. P. Jeyakumar, Y. Jamil, and G. Deivasigamani, "Structural and optical analysis of the role of modifier oxides in multi-component silicate glasses for laser applications," *Eng. Proc.*, vol. 56, no. 1, pp. 0–6, 2023, doi: 10.3390/ASEC2023-15309.

[16] M. Szumera, I. Wacławska, and J. Sułowska, "Thermal properties of MnO_2 and SiO_2 containing phosphate glasses," *Journal of Thermal Analysis and Calorimetry*, vol. 123, no. 2, pp. 1083–1089, Feb. 2016, doi: 10.1007/s10973-015-5010-5.

[17] M. A. Farag, A. Ibrahim, M. Y. Hassaan, and R. M. Ramadan, "Enhancement of structural and optical properties of transparent sodium zinc phosphate glass–ceramics nano composite," *J. Aust. Ceram. Soc.*, vol. 58, no. 2, pp. 653–661, Apr. 2022, doi: 10.1007/s41779-022-00716-3.

[18] A. Samavati et al., "Influence of ZnO nanostructure configuration on tailoring the optical bandgap: Theory and experiment," *Mater. Sci. Eng. B*, vol. 263, Jan. 2021, doi: 10.1016/j.mseb.2020.114811.

[19] S. Ibrahim, A. A. Ali, and A. M. Fathi, "A comprehensive investigation of Bi_2O_3 on the physical, structural, optical, and electrical properties of $K_2O{\cdot}ZnO{\cdot}V_2O_5{\cdot}B_2O_3$ glasses," *Sci. Rep.*, vol. 14, no. 1, Dec. 2024, doi: 10.1038/s41598-024-58567-w.

[20] V. Gupta, S. Kumar, S. K. Arya, R. K. Mishra, and K. Singh, "Functionalization of optical and photoluminescence properties using Li_2O/Na_2O in magnesium phosphate glasses," *Ceram. Int.*, vol. 51, no. 17, pp. 23825–23836, Jul. 2025, doi: 10.1016/j.ceramint.2025.03.071.

[21] F. Ahmadi, R. El-Mallawany, S. Papanikolaou, and P. G. Asteris, "Prediction of optical properties of rare-earth doped phosphate glasses using gene expression programming," *Sci. Rep.*, vol. 14, no. 1, Dec. 2024, doi: 10.1038/s41598-024-66083-0.

[22] K. I. Hussein *et al*., "The investigation of new phosphate–titanite glasses according to optical, physical, and shielding properties," *Crystals*, vol. 12, no. 7, Jul. 2022, doi: 10.3390/cryst12070941.

[23] R. S. Manzan, J. P. Donoso, C. J. Magon, I. D. A. A. Silva, C. Rüssel, and M. Nalin, "Optical and structural studies of Mn^{2+} doped $SbPO_4$–ZnO–PbO glasses," *Journal of the Brazilian Chemical Society*, vol. 26, no. 12, pp. 2607–2614, Dec. 2015, doi: 10.5935/0103-5053.20150289.

[24] K. Adaikalam, S. Hussain, P. Anbu, A. Rajaram, I. Sivanesan, and H. S. Kim, "Eco-friendly facile conversion of waste eggshells into CaO nanoparticles for environmental applications," *Nanomaterials*, vol. 14, no. 20, 2024, doi: 10.3390/nano14201620.

[25] H. Hemmami et al., "Green synthesis of CaO nanoparticles from chicken eggshells: Antibacterial, antifungal, and heavy metal (Pb^{2+}, Cr^{2+}, Cd^{2+} and Hg^{2+}) adsorption properties," *Front. Environ. Sci.*, vol. 12, no. September, pp. 1–17, 2024, doi: 10.3389/fenvs.2024.1450485.